SPATIAL DISCRETIZATION OF THE NESTEROV FIRE RATING INDEX USING MULTISPECTRAL SATELLITE IMAGERY

MILAN ONDERKA[1], IGOR MELICHERČÍK[2]

[1] *Institute of Hydrology, Slovak Academy of Sciences, Bratislava, Slovakia, onderka@uh.savba.sk*
[2] *Faculty of Mathematics, Physics and Informatics, Comenius University, Bratislava, Slovakia*

Fire-risk rating indices are usually based on empirical relationships between pre-event meteorological conditions and the number of observed fire outbreaks. The inherent property of such weather-based indices is that they provide only an area-averaged risk of fire for a given region. This disadvantage can be partially relieved by using remote sensing data. The motivation of this paper is to presents how the Nesterov Index can be merged with the Temperature/Vegetation Dryness Index (TVDI) to create a map of fire risk. The principles of the devised methodology are demonstrated on a set of four LANDSAT 7 scenes taken over Scots pine forests (Pinus Sylvestris L.) in western Slovakia. Our investigation suggests that coupling TVDI with traditional weather-based fire rating indices can become an effective tool for delineating areas prone to fire outbreaks, especially in vast areas with only a limited number of weather stations.

Indexy rizika vzniku lesných požiarov sú zväčša postavené na empirických vzťahoch medzi meteorologickými prvkami pred vznikom požiaru a hláseným počtom vzniknutých lesných požiarov. Vlastnosťou týchto indexov je, že sú schopné poskytnúť iba priemernú hodnotu rizika vzniku lesného požiaru v uvažovanej zalesnenej oblasti. Cieľom tohto článku je demonštrovať jednu z možností použitia údajov z diaľkového prieskumu pre zlepšenie sledovania miest citlivých na vznik požiarov v rozľahlých lesných porastoch. Nesterov index bol prepojený s indexom TVDI (Temperature/Vegetation Dryiness Index), t.j. teplotne-vegetačným indexom sucha, ktorý poskytol informáciu o plošnej distribúcii „zraniteľných" miest. Použili sme štyri satelitné snímky Landsat ETM+ s pokrytím Borských lesov na Záhorskej nížine. Výsledky našej práce ukazujú, že spojenie tradičných metód založených na pozemných meraniach meteorologických prvkov s údajmi z multispektrálnych satelitov by mohlo zlepšiť odhad rizika vzniku požiarov v rozľahlejších oblastiach s nedostatočným pokrytím meteorologických staníc.

Keywords: forest fires, TVDI, Landsat ETM+, Nesterov Index

INTRODUCTION

Several fire-weather indices have been proposed and are currently used worldwide; e.g. the Nesterov Index (Russia), Angstom Index (Scandinavia), Baumgartner Index (Germany), and the Canadian Fire Weather Index. The fundamental feature of these indices is that they are based on a simplified statistical relationships between the reported number of fire events and several weather data characterizing the antecedent weather conditions. Unfortunately, despite their popularity and low computing requirements, weather-based indices can provide only an area-averaged risk of fire, because the only input (weather data) is acquired from point measurements at weather stations.

The climate, topography, and the type of vegetation are recognized as additional factors modulating the fire potential and the rate of spread (Škvarenina et al., 2004). Microclimatic conditions, i.e. temperature of the forest floor along with other favorable conditions (high air temperature, low air humidity, direct solar radiation, and wind) are the main factors facilitating ignition and rapid spread of fire in forests (Tanskanen et al, 2005, Tanskanen et al, 2008; Bowyer & Danson, 2004). There is evidence that fuel moisture content and surface soil moisture are both controlled by the amount of water vapor in the air, rainfall interception, and direct solar heating. Tesař et al. (2006) showed that the density of a forest over-storey directly affects the surface radiation balance and surface temperature of the forest floor. In clearings, the near-surface temperature can be up to several Celsius degrees higher than that in closed canopies. Marthews et al. (2008) studied the effect of gap-size on shallow-soil moisture (5 and 55 mm deep) and surface soil temperature. Surface moisture and temperature of soil in large gaps are controlled primarily by direct solar heating, rainfall, and evaporation. In the case of smaller gaps and closed canopies, solar heating plays a minor role due to the attenuation of solar radiation before reaching the forest floor. As soil and litter both receive a considerable amount of water from precipitation, rainfall remains a vital factor for the moisture status of forest fuels in both smaller gaps and under closed canopies. For instance, Holko et al. (2009) studied the effect of canopy horizontal structure (Norway spruce) in terms of its ability to intercept water. Their findings revealed that gaps, or windows, in a forest canopy exhibit lower rates of rainfall interception. Apart from direct heating, ventilation in gaps and thin forests further enhance the drying out of the litter. The forest microclimate is controlled also by the

species composition and the vertical and horizontal structure of the canopy. Evidence exists that *Pinus sylvestris* may create stand structures allowing wind and sun radiation to penetrate deeper through the tree canopy (Stendberg et al., 1994). Tanskanen et al., 2005 studied the fire ignition potential of *Pinus sylvestris* and *Picea abies* with varying stand structures. The authors reported that stands dominated by *Pinus sylvestris* can be ignited roughly three times more likely than *Picea abies*.

Generally, two types of flammable fuel are considered in fire risk modeling: dead fuel, and live fuel (i.e. green vital leaves, branches etc.). Live fuel has been investigated in terms of its moisture regime (live fuel moisture - LFM) by several authors. Live fuel plays an essential role in crown fire development and the rate of its spread (Peterson et al., 2008; Chuvieco et al., 2008). On the other hand, dead fuel, i.e. dry branches, shrubs and litter, serve as the primary fuel material for human-caused fire ignitions. As Bowyer & Danson (2004) emphasize, LFM varies both in space and time; and is driven primarily by available soil moisture, the type of the underlying soil and most importantly the microclimate within the forest canopy. Dead forest fuel is moistened by precipitation that falls on the forest floor after passing through the canopy (often referred to as "throughfall"). However, the temporal variability of the precipitation is a matter of season, but a high variability occurs within a single storm as well. The distribution of rainfall varies with the storm type, intensity, duration, and time of year (Bedient et al., 2008). Since rainfall is the only source of moisture for forest fuel, spatial variability of precipitation must play an important role in the spatial distribution of fire-prone sites as well.

Fire patrols are traditionally deployed by forest fire managers to assess the risk of forest fires. Conventionally, field surveys of fuel moisture content (FMC) are based on collecting live and dead foliage, drying it in pre-described conditions (Chuvieco et al., 2004), and gravimetrically expressing it as the percentage of evaporated water to the sample's dry weight. While this approach is a valuable source of information, the major drawback of field surveys is that they are time consuming, costly, not feasible in remote areas, and subject to large sampling errors (Danson & Danson, 2004). The spatial representativeness of such point measurements remains questionable.

The advent of remote sensing made it possible to obtain spatial characteristics of forest biomass and surface moisture conditions. Vegetation indices (VIs) derived from remotely sensed data have been used to assess the state of vegetation by diagnosing the spectral features of vegetation in the visible and infra-red region of wavelengths. VIs have found their application in numerous environmental studies: e.g. global climate studies, carbon cycle, evapotranspiration, and soil-moisture monitoring. In fire related studies, VIs derived from satellite data have been used to map extensive areas of dry vegetation. With decreasing moisture in fuel, spectral characteristics of the biomass change in response to water deficiency, since leaf reflectance is controlled mainly by water content, pigments (such as the chlorophyll-a and chlorophyll-b), and dry matter. VIs are particularly sensitive to changes in the content of plant chlorophyll and the leaf area index (LAI), which co-occur with water deficiency (Hardy & Burgan, 1999). Because soil moisture is partially driven by vegetation cover (Verstraetem et al., 2006), VIs become a useful tool for assessing the spatial variability of soil moisture and water deficiency. Nemani et al. (1993) and Park et al. (2004) demonstrated the existence of a close relationship between soil moisture and the Normalized Differential Vegetation Index (NDVI). Wang et al. (2007) investigated the time lag of NDVI behind decreasing soil water content. For humid regions, this time lag may be more than 10 days, while in semi-arid regions NDVI may start to respond to water stress earlier (< 5 days). Significant correlation was found between NDVI and shallow soil moisture at a depth of 50 mm (Wang et al., 2007). Considering that the dead fuel and shallow soil horizons are closely interlinked in their water-energy balance, the reported correlation between NDVI and soil moisture in the most upper horizon of the soil may bear some information on the moisture status of fuels also.

Hernandez-Leal et al. (2004) used the Normalized Differential Vegetation Index (NDVI) scanned by AVHRR-NOAA to track seasonal changes in the vegetation and how this information can be used in assessing the risk of wild fires in Spain. Vidal et al. (1994) used NOAA-AVHRR thermal infrared images and some basic meteorological data to estimate the surface temperature in forests in France. Hernandez et al. (2006) worked toward developing aFire Risk Dynamic Index that would incorporate NDVI into a Static Fire Index, i.e. an index utilizing factors such as proximity to main roads, type of vegetation cover, solar heating, slope, aspect and elevation of the terrain. A similar fire risk zone mapping methodology based on topographic and land-use maps was proposed by Xu et al. (2005). The major drawback of relying merely on VIs in fire-related studies is that VIs may only very slowly respond to water deficiency (Wang et al., 2007). Thermal remote sensing in combination with VIS (visual) and NIR (near-infrared) spectra may capture changes in water deficiency faster than the single use of vegetation indices. The attempt to merge the thermal spectral region with visual and infra-red spectral bands resulted in the Temperature-Vegetation Space, also known as the Temperature-Vegetation Scatterplot. Sandholt et al. (2002) modified the Temperature-Vegetation Scatterplot to identify soil moisture conditions. The modification resulted in the Temperature-Vegetation-Differential Index (TVDI), which is based on relating NDVI to surface temperature in a number of discrete steps.

The goals of this paper are the following:

- to calculate the Nesterov Index for the dates of satellite image acquisition,
- to analyze and process four multispectral images (Landsat ETM+),
- to create maps of the Temperature/Vegetation Dryness Index and to delineate areas prone to forest fire outbreak.

The present methodology is demonstrated on pine forests in Western Slovakia.

Figure 1. Orthophotomap of the investigated area (true color composite RGB, created from Landsat imagery). Location of the weather-stations at Malacky and Senica is indicated with rectangles.

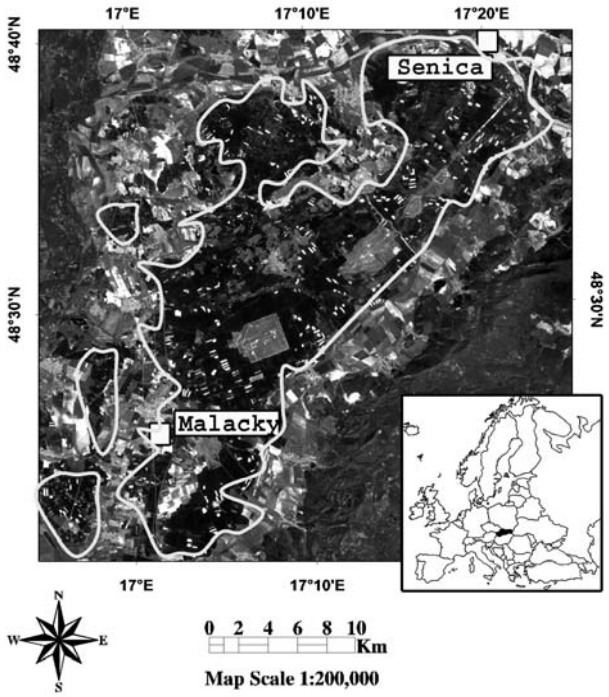

MATERIAL AND METHODS

Study site

The geographical setting of the region of interest is illustrated in Figure 1. This area is located between 48°20'N 17°E and 48°50'N 17°30'E; north of the capital city of Bratislava, Slovakia. This region is dominated by vast patchy areas (totally ~44 000 ha) of coniferous stands (dominated by *Pinus sylvestris* L.) growing on sandy soils (90 % quartz).

Some 35 % of the forested area is formed by natural stands, while the remaining 65 % are occupied by cultural forest plantations. The prevailing north-western winds (annual average: 2.8 m/s) and a low annual precipitation rates (~ 584 mm) make these forests sensitive to fire events. As for the fire statistics in Slovakia, the year 2003 witnessed 872 forest fire events with a burnt area of 1567 ha. This figure is almost three times higher than that of the year 2001, when "only" 311 fire events were reported with 305 hectars of burnt area (European Commission, Report No. 5, 2004).

The growing season lasts ~250 day, and the average air temperature during the peak growing season (June) is 19.6 – 20.2 ºC. The tree under-storey is formed by grasses and herbs (*Festuca ovina agg., Anthoxanthum odoratum , Thymus serpyllum, Acetosella vulgaris, Calamagrostis epigejos, Mycelis muralis, Hypericum perforatum*); mosses are dominated mainly by *Plerozium schreberi*, forming continuous carpets on the forest floor in some areas; lichens; with shrubs of *Quercus petraea agg., Petula pendula* Roth., and young *Pinus sylvestris* L., (Mikuška, 2005).

Nesterov Index

In 1949, Nesterov (Shetinsky, 1994) proposed a fire-risk rating index to be used in the continental former Soviet Union. This index establishes a range of discrete fire risk levels. The Nesterov Index is calculated as:

$$NI = \sum_{i=1}^{w} \left(T_i - T_i^{dew}\right) T_i \,, \tag{1}$$

where

NI denotes the Nesterov Index,
w is the number of days since the last rainfall exceeding 3 mm per day,
T_i is the temperature (°C) on a given day,
T_i^{dew} is the dew point temperature (°C).

The intrinsic characteristic of the Nesterov Index is that it is reset to "zero" when daily rainfall exceeds 3 mm per day (Shetinsky, 1994). Figure 2 illustrates the workings of the Nesterov Index. After each rainfall exceeding 3 mm per day (the upper horizontal axis in Fig. 2), the index drops to zero. The original risk levels proposed by Nesterov were classified as follows:

- NI < 300 no risk,
- 301 < NI < 1000 low risk,
- 1001 < NI < 4000 medium risk,
- 4001 < NI < 10 000 high risk,
- NI > 10 000 extremely high risk.

NI was calculated for the four dates of satellite image acquisition, e.g. May 1, 2000; May 14, 2000; August 2, 2000; and August 24, 2002. Input data were acquired from the databases of the Slovak Hydrometeorological Institute.

Figure 2. Daily series of rainfall and the Nesterov Index "NI" (June – October, 2003, Senica Station). Minimum rainfall (dashed line) at which the Nesterov Index is reset.

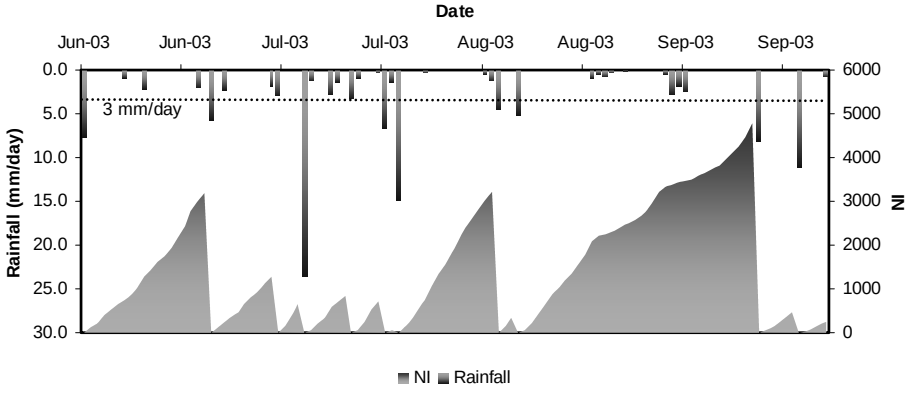

Satellite image processing

The satellite images used in this study were acquired on days with clear skies. Four Landsat ETM+ images were processed and analyzed. The dates of acquisition were: May 1, 2000; May 14, 2000; August 2, 2000; and August 24, 2002. Supervised classification was used to create maps of forest-only areas in the ENVI 4.3. software package. Landsat ETM+ scenes contain three visible bands (Band 1 through Band 3), two infrared bands (Bands 4, 5 and 7) with a spatial resolution of 30 meters, and one thermal band with a resolution of 60 meters (Band 6 – operating in the spectral region between 10.4 and 12.5 μm), (see Landsat Handbook, http://landsathandbook.gsfc.nasa.gov/handbook.html). A map of the forest-only areas was extracted from raw satellite images by the supervised classification algorithm based on the maximum likelihood classification technique. Training pixels were collected from pre-selected regions of interest (ROIs) using all three visual bands (R, G, B), one near-infrared band (TM4) and the thermal band (TM6). The created classified image was used for binary masking to exclude areas other than coniferous forests from analysis.

Temperature/Vegetation Dryness Index

To establish a spatially variable attribute of the Nesterov Index we focused on the work of Sandholt et al., 2002. The concept of "Ts-Vegetation Space" was originally proposed to assess the soil moisture status of vegetation. In principle, the Ts-Vegetation Space represents a scatter-plot of remotely sensed surface temperature and NDVI collected from a sample area with a broad range of moisture conditions. Goward et al. (1985) demonstrated a strong negative relationship between radiometric surface temperature and NDVI; which was explained by evaporative cooling of the green live biomass. When surface conditions become drier, vegetated areas transpire less water, and, when a drought period prevails for a sufficiently long time, NDVI values decrease and the surface temperature tends to increase due to hindered evaporative cooling. Figure 3 explains the Temperature/Vegetation Dryness Index (TVDI) in detail. Calculation of the Temperature/Vegetation Dryness index is based on the following equation:

$$TVDI = \frac{T_S - T_{S\_min}}{a + b \times NDVI - T_{S\_min}}, \quad (2)$$

where

T_S is the surface temperature,
T_{S_min} is the minimum surface temperature in the triangle necessary to define the "wet edge",
NDVI is the normalized differencial vegetation index,
a and b are parameters derived from a linear fit to $T_{S\_max} = a + b \times NDVI$.

Note that the triangle in Figure 3 is enclosed by two curves: the upper curve, called the "dry edge"; and the lower curve, called the "wet edge". The "wet edge" and "dry edge" in the triangle (Fig. 3) represent the TVDI boundary values. TVDI equals zero on the wet edge, and unity (1) on the dry edge. All TVDI values between these two edges may therefore take values only in the range 0 – 1.

Figure 3. Explanatory plot of the Temperature/Vegetation Dryness Index (adopted and modified from Sandholt et al., 2002).

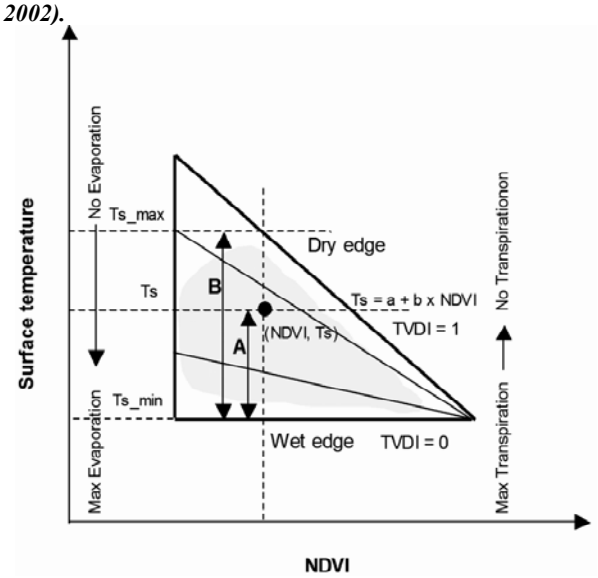

Retrieval of Normalized Differential Vegetation Index

NDVI was calculated as the difference between NIR and Red spectral regions, normalized to the sum of the NIR and Red spectral band (Eq. 3):

$$NDVI = \frac{\rho_{NIR} - \rho_{Red}}{\rho_{NIR} + \rho_{Red}}, \quad (3)$$

where

ρ_{NIR} is the spectral radiance detected in the near-infrared band (760 – 900 nm),
ρ_{Red} is the spectral radiance detected in the red band (630 – 690 nm).

The range of NDVI values can yield values only between –1 and 1. As a rule of thumb, the higher NDVI values characterize green and healthy biomass. For healthy coniferous forests, NDVI may be within the range of 0.2 – 0.8, depending on the sensor view angle and the Sun position (Table 3).

Land Surface Temperature

Brightness temperatures (temperature of surface as "seen" by the satellite sensor) were extracted from the processed satellite scenes following the conventional algorithms for surface temperature retrieval (see Landsat Handbook)

$$T_S = \frac{k_2}{ln\left(\frac{\varepsilon \times k_1}{R_C} + 1\right)}, \quad (4)$$

where

T_S is the surface temperature (K),
k_1, k_2 are calibration constants ($k_1 = 666.09$ W/m^2 sr μm, $k_2 = 1282.71$ K),
R_C is the at-sensor radiance.

The thermal data were corrected for atmospheric effects. This step is essential in absolute temperature studies (Barsi et al., 2003). The Radiative Transfer Model available as a web-based tool (Barsi et al., 2003; http://atmcorr.gsfc.nasa.gov/)

was used to estimate the transmission, upwelling and downwelling radiance. The input data for the Radiative Transfer Model were acquired at a weather station at Malacky. It would be outside the scope of this study to go into much detail concerning the temperature retrieval mechanism, and therefore the reader is encouraged to read appropriate literature covering this topic (e.g., Barsi et al., 2003; Sobrino et al., 1991a; Sobrino et al., 1991b; Qin et al., 2001, to cite just a few).

Table 1. Nesterov Index (NI) calculated for the dates of satellite image acquisition for the two weather stations ($NI_{Malacky}$ and NI_{Senica}). The average index for the whole region (Malacky + Senica) is calculated as an arithmetic average $\overline{NI}$.

Date	$NI_{Malacky}$	NI_{Senica}	$^{*}\overline{NI}$
May 14, 2000	5156	1224	3190.0
August 2, 2000	404	351	377.5
May 1, 2001	1175	920	1047.5
August 24, 2002	731	1252	991.5

Note: $^{*}\overline{NI} = \frac{1}{2}\left(NI_{Malacky} + NI_{Senica}\right)$

Table 2. Earth-Sun position characteristics on the acquisition dates, and TVDI parameters (a and b in Eq. 2).

Date	Azimuth	Sun Elevation	a	b	T_{s_min} (K)
May 1, 2001	148.2	52.8	305.83	–25.7	299.2
May 14, 2000	145.1	57.4	312.43	–15.9	298.9
August 2, 2000	143.6	54.0	309.48	–14.2	302.0
August 24, 2002	147.8	48.3	304.42	–13.3	299.8

RESULTS

Four Landsat ETM+ images were used to derive the TVDI index. Sub-images of the distribution of TVDI on the dates of satellite overpass are depicted in Figure 5. Note that the TVDI index is highly variable between the four investigated images. As shown in Table 1, NI may differ between two weather stations and may be quite different despite the relative short distance between them (~35 km). This difference may be explained by the fact that precipitation is a highly variable phenomenon; i.e. there may be a summer storm formation in one area, while a few kilometers away there is no rainfall. This is evident in Table 1 listing the calculated Nesterov Index for the analyzed dates. For example, on May 14, 2000, at the Malacky weather station the NI was 5156, while at the Senica Station the NI was 1224. Therefore, relying merely on the NI derived from only one weather station may lead to misleading levels of fire-risk if the spatial character of the index is not taken into account. Using the Nesterov Index (or any other fire rating index based on meteorological data) in synergy with the TVDI may be beneficial in terms of assigning each pixel in a satellite image, an intrinsic fire risk value (Fig. 5). Figure 4 shows the TVDI triangle created from the image-derived data and using Eq. 2. The unknown parameters (a, b, T_{s_min}) in Eq. 2 were identified iteratively (using Solver MS Excel) after setting the objective function (TVDI_max) equal to unity. Note that the TVDI index can yield values only in the range 0 – 1. Dividing this interval into three equal subintervals (0 – 0.33; 0.33 – 0.66; and 0.66 – 1.0) made it possible to roughly differentiate between pixels with a "low" –

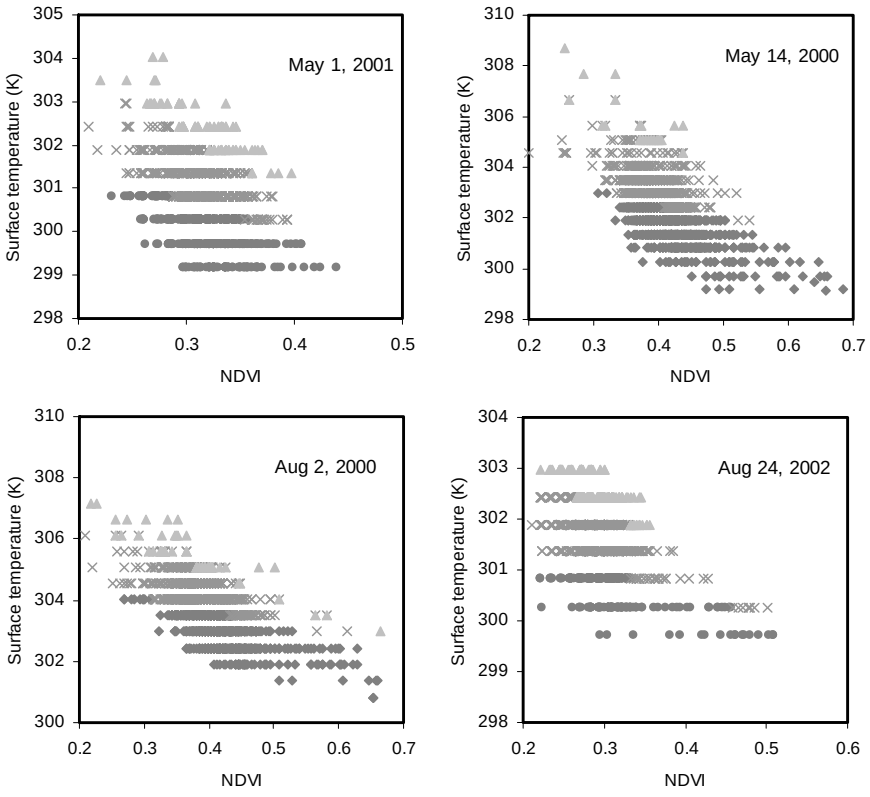

Figure 4. TVDI scatterplots for the dates of image acquisition (May 1, 2001, May 14, 2000, August 2, 2000, August 24, 2002).

Legend:
- ***TVDI ∈ (0 – 0.33)***
- ***TVDI ∈ (0.33 – 0.66)***
- ***TVDI ∈ (0.66 – 1.0)***

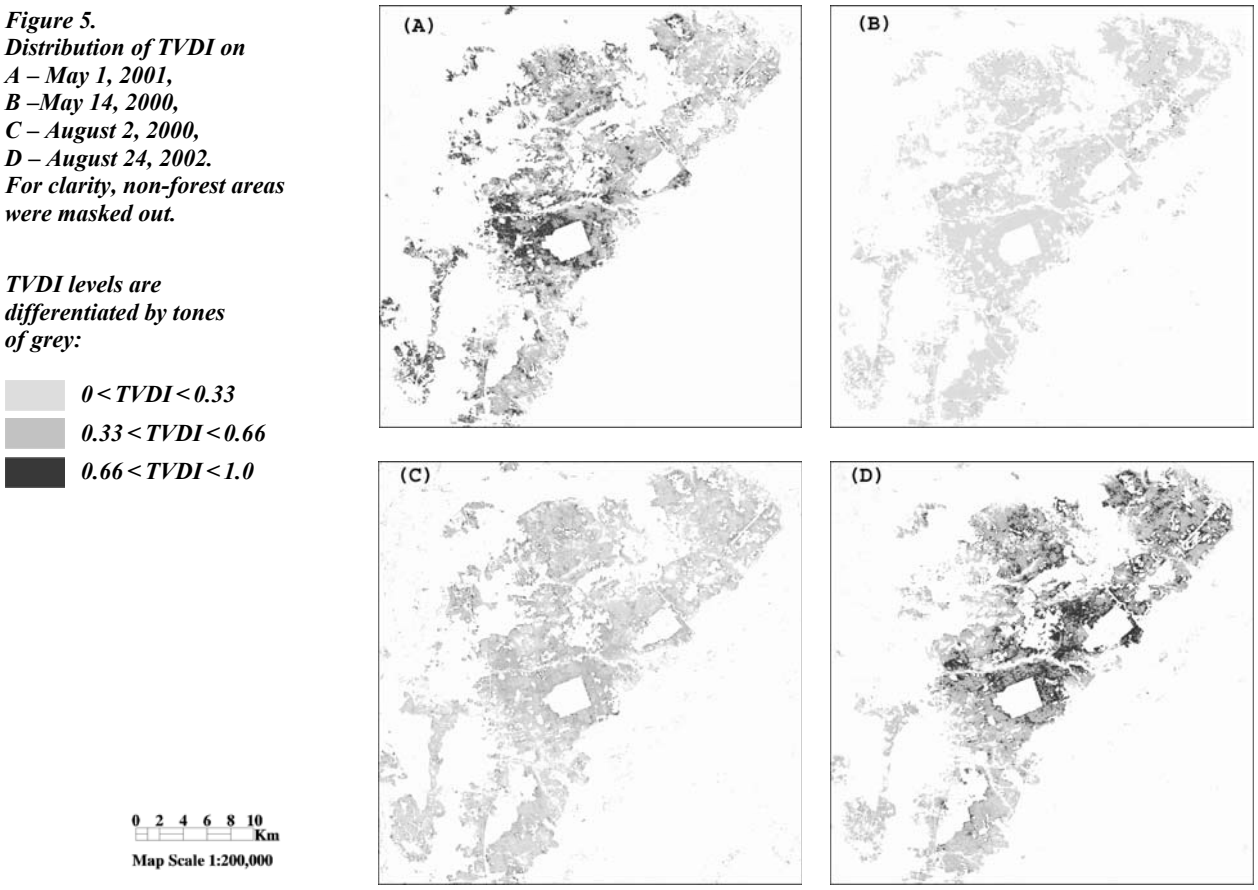

Figure 5.
Distribution of TVDI on
A – May 1, 2001,
B –May 14, 2000,
C – August 2, 2000,
D – August 24, 2002.
For clarity, non-forest areas were masked out.

TVDI levels are differentiated by tones of grey:

"moderate" and "high" risk of fire outbreak. In addition, calculating the Nesterov Index for the dates of the satellite image acquisition enabled us to assign to the NI a spatial attribute when used with the spatially varying TVDI. Sites with higher TVDI show where the risk of fire occurrence is more "probable". Linking this value to the TVDI map calculated for the May 1, 2001 (Fig. 5) shows that the risk was not equally distributed over the investigated area.

CONCLUSIONS

Four Landsat ETM+ images were used to demonstrate the presented methodology – i.e. using TVDI to assign the Nesterov Index a spatially variable attribute. Sub-images of the area of interest (Fig. 5 A–D) show the distribution of the TVDI on the dates of satellite overpass. Note that the TVDI index is highly variable. The spatial variability is apparent especially in Figure 5 B–C, where the higher TVDI values are shifted northerly (Fig. 5 B) and southerly (Fig. 5 C). The rest of the TVDI maps (Fig. 5 A, D) seem to be invariant with respect to the TVDI values. Despite the apparent homogeneousness of the TVDI in these two images, there is still some variation in the level of TVDI, albeit only within a narrower range, that is lost due to the use of only three discrete levels of TVDI (0 – 0.33, 0.33 – 0.66, 0.66 – 1.0). Moreover, closer examination revealed that higher values of TVDI are present at forest edges. This is not surprising, because experimental evidence exists showing that a canopy located at forest edges dries more quickly than the canopy within the forest owing to the enhanced evapotranspiration and decreased water storage near forest edges (Klaassen et al., 1996). Enhanced ventilation at the forest edges may play a role also. However, suspicion may arise in terms of incorrect interpretation of the forest edge effect; i.e. misclassification of mixed pixels. Therefore, attention should be paid to the issue of sub-image analysis also. In general, the higher value of the TVDI suggests drier conditions within the analyzed pixels, hence a higher chance of fire outbreak exists in areas where the TVDI exhibits elevated values. However, it should be noted here that TVDI values are independent of the Nesterov Index (or any other fire risk rating index derived from weather data). Similar values of TVDI may be obtained on two days with different values of the Nesterov Index.

The presented methodology may find its application in areas where weather-stations are installed over large distances. In such instances, the calculated Nesterov Index (or any other weather-based index) may yield misleading results in terms of its spatial representativenes. Remotely sensed data may be used as a supplementary attribute useful for delineating sites with dry fuel conditions.

Acknowledgment

The authors wish to express their gratitude to the EU project GOCE 037063 "GEO-BENE", and MVTS (Assessment of evapotranspiration and soil-vegetation dryness in forested areas of Slovakia by multispectral, thermal and SAR satellite imagery), for necessary funding. Satellite images used in this study were acquired from the European Space Agency and the U.S. Geological Survey.

REFERENCES

Barsi, J. A.–Schott, J. R.–Palluconi, F.D.–Helder, S.J.–Hook, S.J. et al., 2003, Landsat TM and ETM + Thermal Band Calibration, Canadian Journal of Remote Sensing, 28, 141–153.

Bastiaanssen, W.G.M., 2000, SEBAL-based sensible and latent heat fluxes in the irrigated Gediz Basin, Turkey, Journal of Hydrology, 229, 87–100.

Bedient, P.B., Hubert, W.C., Vieux, B.E., 2008, Hydrology and flood plain analysis. Forth edition. Pearson International Edition. Prentice-Hall Inc. ISBN 13:978-0-13-242286-4, pp 29.

Bowyer, P.–Danson, F.M., 2004, Sensitivity of spectral reflectance to variation in live fuel moisture content at leaf and canopy level. Remote Sensing of Environment, 92, 297–308.

Chuvieco, E.–Cucero, D.–Riano, D.–Martin, P.–Martinez-Vega, J., de la Riva, J., Perez, F., 2004, Combining NDVI and surface temperature for the estimation of fuel moisture content in forest fire rating, Remote Sensing of Environment, 92, 322–331.

Danson F. M., Bowyer P. (2004). Estimating live fuel moisture content from remotely sensed reflectance. Remote Sensing of Environment, 92, 309–321.

European Commission Report No. 5. Forest Fires in Europe 2004. S.P.I.05.147 EN, 30 pp.

Goward, S.N.–Cruickshanks, G.D.–Hope, A.S., 1985, Observed relation between thermal emission and reflected spectral radiance of a complex vegetated landscape, Remote Sensing of Environment, 18, 137–146.

Hardy, C.C.–Burgan, R.E., 1999, Evaluation of NDVI for monitoring live fuel moisture in three vegetation types of the western U.S. Photogrammetric Engineering and Remote Sensing, 65, 603–610.

Hernandez-Leal, P.A.–Arbelo, M.–Gonzalez-Calvo, A., 2006, Fire risk assessment using satellite data. Advances in Space Research, 37, 741–746.

Holko, L.–Škvarenina, J.–Kostka, Z.–Frič, M.–Staron, J., 2009, Impact of spruce forest on rainfall interception and seasonal snow cover evolution in the Western Tatra Mountains, Slovakia, Biologia, 64(3), 594–599.

Klaassen, W.–Lankreijer, H.J.M.–Veen, A.W.L., 1996, Rainfall interception near a forest edge. Journal of Hydrology, 185, 349–361.

Landsat Handbook, http://landsathandbook.gsfc.nasa.gov/handbook.html

Marthews, T.R.–Burslem, D.F.R.P.–Paton, S.R.–Yanguez, F.–Mullins, C.E., 2008, Soil drying in a tropical forest: Three distinct environments controlled by gap size, Ecological Modelling, 216, 396–384.

Mikuška, B., 2005, Syntaxonomy of the cultural oak-pine forests in the Zahosrska nizina Lowland. Bull. Slov. Bot. Society, Bratislava, Slovakia, 27, 157–169.

Nemani, R.–Pierce, L.–Running, S.N.–Goward, S.N., 1993, Developing satellite-derived estimates of surface moisture status. Journal of Applied Meterology, 32, 548–557.

Park, S.–Feddema, J.J.–Egbert, S.L., 2004, Impacts of hydrologic soil properties on drought detection with MODIS thermal data. Remote Sensing of Environment, 89, 53–62.

Peterson, S.H.–Roberts, D.A.–Dennison, P.E., 2008, Mapping live fuel moisture with MODIS data: A multiple regressin approach, Remote Sensing of Environment, 112, 4272–4284.

Sandholt, I.–Rasmussen, K.–Andersen, J., 2002, A simple interpretation of the surface temperature/vegetation index space for assessment of surface moisture status, Remote Sensing of Environment, 79, 213–224.

Shetinsky, E.A., 1994, Protection of forests and forest pyrology. Ecology, Moscow (in Russian), 209 p.

Škvarenina, J.–Mindáš, J.–Holécy, J.–Tuček J. (2004). An analysis of the meteorological conditions during two largest forest fire events in the Slovak Paradise National Park. Meteorological Journal, 7, 167–171.

Sobrino, J.A.–Caselles, V., 1991a, A methodology for obtaining the crop temperature from NOAA-9 AVHRR data. International Journal of Remote Sensing, 12, 2461–2475.

Sobrino, J.A.–Cull, C.–Caselles, V., 1991b, Atmospheric correction for land surface temperature using NOAA-11 AVHRR channels 4 and 5. Remote Sensing of Environment, 38, 19–34.

Qin, Z.–Berliner, P.–Karnieli, A., 2001, A mono-window algorithm for retrieving land surface temperature from Landsat TM data and its application to Israel-Egypt border region. International Journal of Remote Sensing, 22, 3719–3746.

Tanskanen, H.–Venalainen, A.–Puttonen, P.–Granstrom A., 2005, Impact of stand structure on surface fire ignition potential in Picea abies and Pinus sylvestris forests in southern Finland. Can J. For. Res., 35, 410–420.

Tanskanen, H.–Venalainen, A., 2008, The relationship between fire activity and fire weather indices at different stages of the growing season in Finland. Boreal Environment Research, 13, 285–302.

Tesař, M.–Šír, M.–Lichner, L.–Zelenková, E., 2006, Influence of vegetation cover on thermal regime of mountainous catchments. Biologia, 61/Suppl. 19, 311–314.

Vertraeten, W.W.–Veroustraete, F.–van der Sande, C.– Grootaers, I.–Feyen, J., 2006, Soil mositure retrieval using thermal inertia, determined with visible and thermal spaceborne data, validated for European forests, Remote Sensing of Environment, 101(3), 299–314.

Vidal, A.–Pinglo, F.–Durand, H. et al., 1994, Evaluation of a temporal fire risk index in Mediterranean forests from NOAA thermal IR. Remote Sensing of Environment, 49, 296–303.

Wang, X.–Xie, H.–Guan, H.–Zhou, X., 2007, Different responses of MODIS-derived NDVI to root-zone soil moisture in semi-arid and humid regions. Journal of Hydrology. 340, 12–24.

Xu, D.–Dai, L.–Shao, G.–Tang, L.–Wang, H., 2005, Forest fire risk zone mapping from satellite images and GIS for Baihe Forestry Bureau, Jilin, China, Journal of Forestry Research, 16, 169–174.